HNUE JOURNAL OF SCIENCE DOI: 10.18173/2354-1059.2022-0025
Natural Sciences 2022, Volume 67, Issue 2, pp. 86-93
This paper is available online at http://stdb.hnue.edu.vn

ENHANCE A PHOTOCATALYTIC ACTIVITY ON Ag_3PO_4 BY Ag/Ag_3PO_4 COMPOSITES

Nguyen Manh Hung[1], Dao Viet Thang[1], Nguyen Thi Dieu Thu[1], Ho Quynh Anh[1], Nguyen Cao Khang[2,*], Le Thi Mai Oanh[2], Pham Do Chung[2], Nguyen Thi Nhung[2] and Lam Thi Hang[3]

[1]*Department of Physics, Hanoi University of Mining and Geology*
[2]*Faculty of Physics, Hanoi National University of Education*
[3]*Department of Physics, Hanoi University of Natural Resources and Environment*

Abstract. In this study, we investigated the formation and influence of Ag particles on the physical properties and photocatalytic performance of Ag_3PO_4 photocatalysts when Ag particles adhered to the Ag_3PO_4 surface. The material is prepared by a simple precipitation method with illumination. The properties of the materials were investigated by X-ray diffraction (XRD), Raman scattering, scanning electron microscopy (SEM), UV-vis absorption, and the photocatalytic ability to decompose organic solutions. The results show the vibrational change of the $[PO_4]$ group in the structure presented in the Raman scattering spectrum highest RhB decomposition. The experimental results indicated that the Ag/Ag_3PO_4 showed highly efficient and stable photocatalytic activity under visible light irradiation. The Ag/Ag_3PO_4 sample with the Ag^+/PO_4^{3-} the ratio of 3.6/1 gave efficiency when stimulated with visible light of Xenon lamps. This sample degraded almost completely to RhB in 10 ppm solution after 15 min of illumination, with a decomposition rate of 0.241 min^{-1}.

Keywords: photocatalytic, silver orthophosphate, Rhodamine B, Ag/Ag_3PO_4.

1. Introduction

In recent years, 2D materials based on nanostructured carbon materials such as carbon nanotubes (CNTs), graphene, and graphene oxide with environmental cleaning applications have increased and attracted the research attention of scientists [1]. With porous structure, large surface area, and special physico-chemical properties, carbon nanomaterials have adsorption capacity and remove water pollutants such as heavy metals or toxic organic matter [2]. Besides the above-mentioned carbon nanomaterials, silver phosphate (Ag_3PO_4) is also noticed after the 2010 discovery of its photocatalytic ability in the visible light region. This material has a small optical band gap (Eg = 2.43 eV), high quantum efficiency, and outstanding photooxidation ability [3, 4].

Received June 14, 2022. Revised June 23, 2022. Accepted June 30, 2022.
Contact Nguyen Cao Khang, e-mail address: khangnc@hnue.edu.vn

Although Ag_3PO_4 (APO) has great potential in the field of environmental remediation and renewable energy, APO still has the limitation of consuming a large amount of silver metal if widely used, leading to increased costs for photocatalysis [5]. In addition, during the photocatalytic activity, Ag^+ ions in the APO crystal lattice are susceptible to metallization when receiving electrons, leading to unwanted and uncontrolled corrosion of APO [6, 7]. As a result, the structure of the material is destroyed over time and the photocatalytic activity decreases. These disadvantages lead to the low efficiency of large-scale APO applications, which is still a challenge for researchers. Therefore, besides finding solutions to improve the surface area, the researchers also focused on reducing the cost of APO photocatalysts and increasing the structural stability of the materials by simple, low-cost methods such as combining APO with other semiconductors [7-11], adjusting the ratio of Ag^+ and PO_4^{3-}, or doping with suitable ions [12-14] both to increase the electron-hole pair lifetime through charge transfer and reduce the cost of the photocatalyst.

In this study, we used the radical $[PO_4]^{3-}$ in the initial precursor $K_2HPO_4.3H_2O$. The Ag^+/PO_4^{3-} ratio is calculated so that the excess Ag^+ compared to PO_4^{3-} in the reaction forms Ag_3PO_4. Excess Ag^+ will be reduced by light to form Ag^0 atoms attached to the Ag_3PO_4 surface to increase photocatalytic efficiency. Rhodamine B (RhB) in an aqueous solution was used as a photocatalytic reagent for Ag/Ag_3PO_4 materials, using excitation Xenon lamp light. The photocatalytic efficiency of Ag/Ag_3PO_4 with RhB was evaluated and explained based on experimental results.

2. Content

2.1. Experiments

Ag/Ag_3PO_4 materials were prepared by direct precipitation method combined with Ag^+ ion reduction by incandescent light. The material fabrication process is carried out as follows: First, slowly add 5 mL of 0.3 M K_2HPO_4 solution to 15.5 mL of 0.3 M $AgNO_3$ solution. The drip process is continuously magnetically stirred at room temperature. In the next step, after forming the Ag_3PO_4 precipitate, the reaction system is illuminated with light for 3 hours to reduce excess Ag^+ ions to form Ag^0 atoms. Finally, the precipitate was filtered, washed, and dried at 100 °C to obtain a yellow powder product. The system of samples was fabricated to change the volume of the $AgNO_3$ solution to create excess Ag^+ atoms in the reaction. The samples were fabricated with the Ag^+/PO_4^{3-} the molar ratio of 3/1; 3.2/1; 3.4/1; 3.6/1; 3.8/1 denoted respectively as APO; APO3.2; APO3.4, APO3.6, and APO3.8.

The photocatalysis experiment was conducted as follows: First, dissolve 0.6 grams of Ag/APO sample in 30 mL of H_2O, stirring for 30 minutes at room temperature. Next, this solution was poured into 30 mL of 20 ppm RhB and stirred in the absence of light for 30 min to reach a saturated adsorption state and the RhB concentration was diluted to 10 ppm. Finally, place the solution under a Xenon lamp (300 W power) after filtering the ultraviolet light. After the specified time intervals, about 4 mL of RhB solution were taken and centrifuged (4000 rpm for 10 min) to remove Ag/APO powder. After centrifugation,

the concentration of RhB solution was determined through transmission spectrometry with an excitation wavelength of 552 nm on a Jassco L1.

The structure of the materials was investigated by X-ray diffraction (XRD) measurements made on the D8-Advance measuring system with Cu-Kα radiation (λ = 1.54064 Å), 2θ angle from 20° to 90°. The surface morphology of the material was obtained by scanning electron microscopy (SEM) measurement performed on the JED-2300 measuring system. Raman spectroscopy was performed on a Horiba LabRam HR Evolution measuring system with a laser wavelength of 532 nm. UV-vis absorption spectroscopy was performed on a Jasco V670 measuring system.

2.2. Results and discussion

The crystal structures of the Ag/APO samples were determined by XRD. Figure 1a is the XRD diagram of APO, and Ag/APO samples with different Ag^+/PO_4^{3-} molar ratios in the precursor solution. The diffraction patterns of all samples are consistent with JCPDS standard tag No. 06-0505 and have no strange peaks, showing that the samples are APO with body-centered cubic structure with space group P4-3n. Sharp diffraction peaks with small full width at half maximum (FWHM) indicate that the samples crystallize well. The lattice constant and crystal size (D_{XRD}) was determined by determining the peak position (angle 2θ), lattice plane, and FWHM combine using UnitCell software and the Debye Sherrer formula. The results show that the lattice constants and crystal size are a = b = c ~ 5.989 Å and D_{XRD} ~ 45 nm for the APO sample. This result is relatively consistent with previous studies [5, 15]. The position of the peak (210) of the different samples is enlarged and shown in Figure 1b. Observation in Figure 1b shows that the peak position (210) has a slight shift towards the large 2θ angle when the Ag^+/APO ratio increases. Therefore, when the Ag^+/APO ratio increases, the lattice constants are reduced but not significantly.

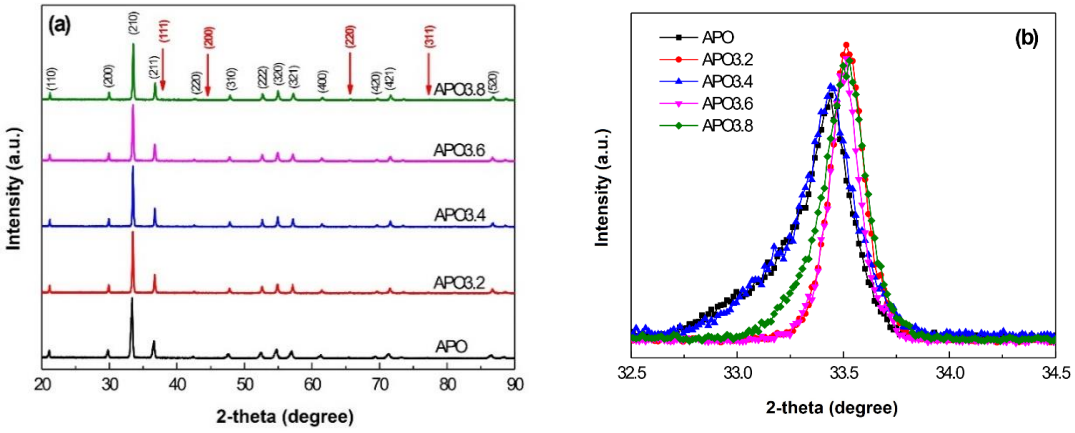

Figure 1. XRD pattern of the Ag/APO sample system (a) and magnified diffraction peak (210) (b)

On the XRD plot of the Ag/APO samples, the Ag characteristic peaks (111), (200), (220), or (311) (points indicated by arrows in Figure 1a are not observed. The failure to observe the characteristic diffraction peaks of Ag may be due to the small amount of Ag

formed in the samples. To confirm this further, we will observe the surface morphology of the material through SEM.

Figure 2 is the SEM image of the Ag/APO samples. Observation in Figure 2 shows that the Ag/APO samples are all granular, about 300 - 600 nm in diameter. The APO sample has a fairly uniform particle size and seems to be larger than that of the Ag/APO samples, the particle size decreases when the Ag/APO ratio increases. In addition, in Ag/APO samples, we also observed that there are small particles attached to the surface of large particles. The number of small particles adhering was greater in the samples with the higher Ag/APO ratio as well as the less uniform large particles. We think that the small particles are Ag particles formed during the illumination process that adheres to the surface of the large particles is Ag_3PO_4.

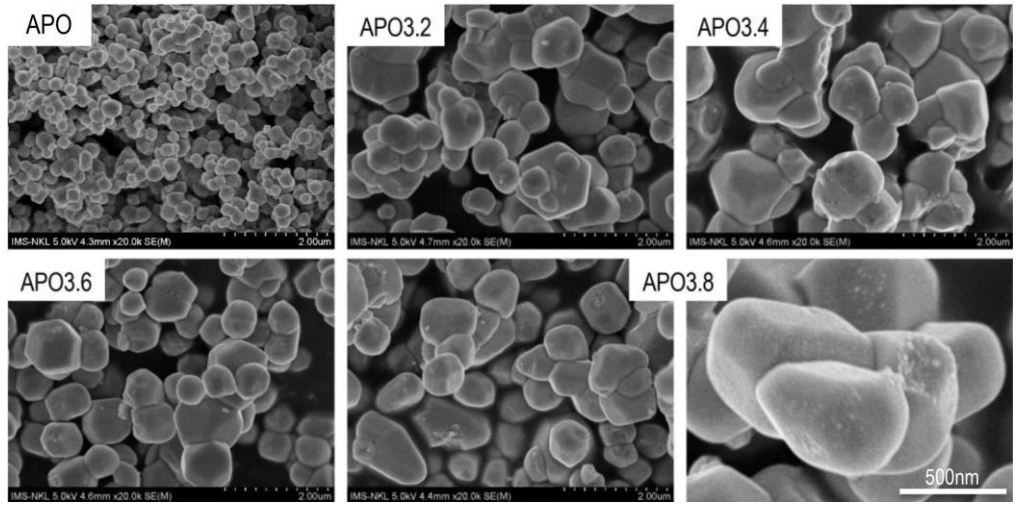

Figure 2. SEM images of Ag/APO samples

Raman spectra of the Ag/APO samples in Figure 3a give information about the bonding and oscillations in the crystal lattice. In the wave number range 100 - 1100 cm^{-1}, the scattering spectrum of the samples appeared 9 peaks of vibration at frequencies 147, 238, 405, 563, 723, 908, 958, 1001, and 1050 cm^{-1}. Most of the oscillation peaks are of low intensity except the one at 908 cm^{-1}. The spectral peak at 908 cm^{-1} is assigned to the symmetric stretching vibration A_1, while the spectral peak at 958 and 1001 cm^{-1} is assigned to the asymmetric stretching vibration T_2 of the tetrahedron [PO_4]. The spectral peaks at 405 and 563 cm^{-1} are E-symmetric and asymmetrical bending T_2 and the peak at 238 cm^{-1} is a rotational or translational oscillation T_2 of the [PO_4] group [16]. The spectral peak observed at 723 cm^{-1} is attributed to either a symmetrical stretching oscillation of the O-P-O bonds or to a coherent oscillation [17]. The spectral peaks at 238 and 1001 cm^{-1} have an intensity that increases with the Ag/APO ratio. The change in intensity of the asymmetric peaks may have added Ag bonds in the structure of Ag_3PO_4, which is also consistent with previous studies [16, 18]. Figure 3b shows the peak detail at 908 cm^{-1} of the Gaussian fit sample including three peaks of 908, 901, and 919 cm^{-1}. They can be assigned to the symmetric stretching vibration (A_1) and two asymmetric stretching vibrations (T_2) of the [PO_4] group [16], respectively. However, in sample APO3.6, position 908 cm^{-1} has only one A_1 symmetry peak. The T_2 asymmetric double-peak change shows that there is a small change (about 11 cm^{-1}) in the binding and structural

vibrations between the APO and Ag/APO samples. This result is consistent with the results from the SEM image, confirming the appearance of Ag particles attached to the Ag_3PO_4 particles.

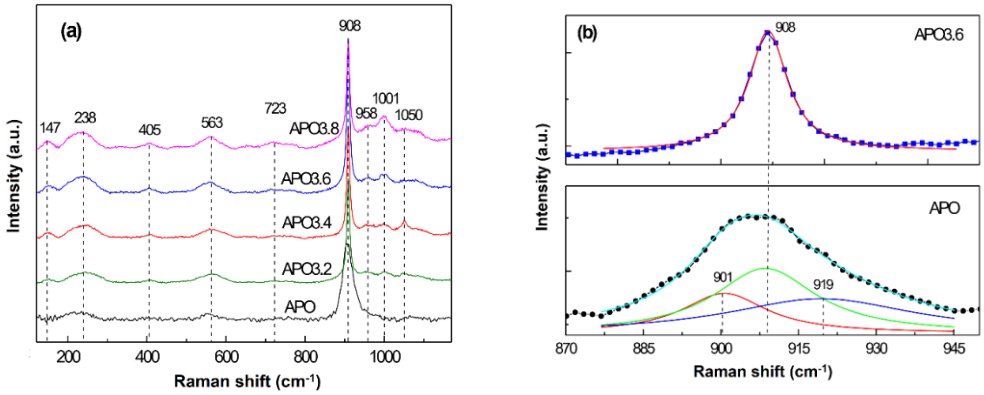

Figure 3. Raman scattering spectra of Ag/APO samples

UV-Vis absorption spectroscopy was performed to determine the energy band gap of the synthesized APO and is shown in Figure 4a. All samples exhibit strong absorption at wavelengths shorter than 520 nm, demonstrating that visible light can be used for photocatalysis. Using the Kubelka-Munk function, the energy bandgap Eg can be determined from the graph representing $(\alpha h\nu)^{1/2}$ by photon energy (hc/λ) for an indirect transition semiconductor as shown in Figure 4b. The calculated results, the band gap of the APO and the APO3.8 sample is 2.40 eV and, 2.36 eV, respectively.

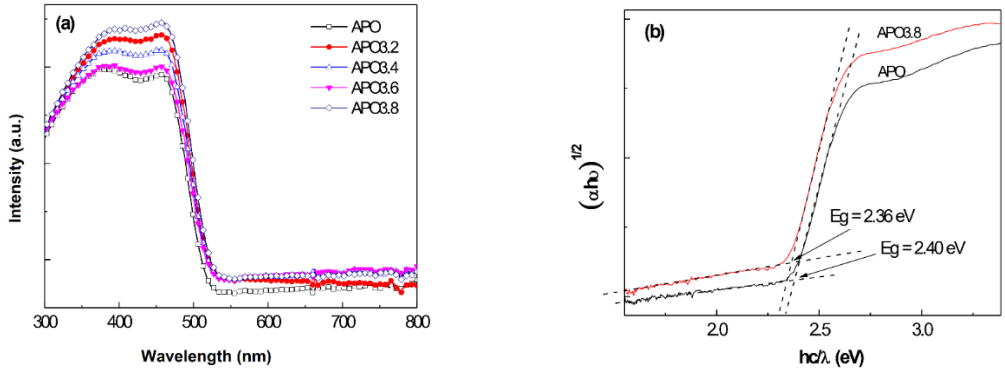

Figure 4. a) UV-vis absorption spectrum of Ag/APO samples, b) The curve represents $(\alpha h\nu)^{1/2}$ in terms of photon energy (hc/λ)

The photocatalytic ability of the Ag/APO samples under visible light was evaluated through the 10 ppm RhB decomposition under the Xenon lamp illumination. Xenon lamp used in the experiment has a luminous intensity of 180 W/m^2. Figure 5a shows curves representing the relative C/C_0 ratio of RhB remaining in solution over time. Before illumination, the solutions were magnetically stirred in the dark for 30 min to achieve a saturated adsorption state. The results showed that the synthesized Ag/APO material rapidly adsorbed about 10% of RhB and reached equilibrium in less than 10 min.

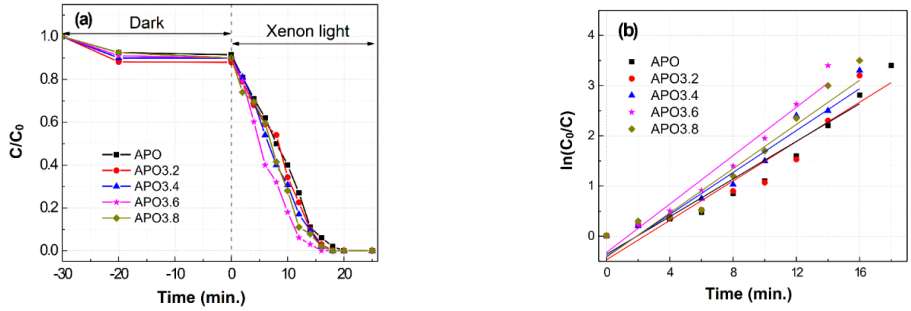

Figure 5. a) Photocatalytic activity and b) reaction rate of RhB-degrading Ag/APO samples in solution under visible light of Xenon lamp

All Ag/APO samples showed strong photocatalytic performance, especially for sample APO3.6, which completely decomposed RhB in 15 min. Using a first-order kinetic model to determine the photocatalytic reaction rate with about 2% of error, $ln(C_0/C) = kt$, where the rate constant k can be determined from the slope of the linear relationship in the diagram. $ln(C_0/C)$ compared with the reaction time (Figure 5b). Sample APO has a reaction rate constant $k \sim 0.187$ min^{-1}; samples APO3.2, APO3.4, APO3.6, APO3.8 have reaction rate constants of k (min^{-1}) ~ 0.196, respectively; 0.209; 0.241 and 0.220. In Ag/APO samples, the reaction rate constant tends to increase and is the highest with sample APO3.6.

In the Ag/APO samples, Ag_3PO_4 and Ag are both able to absorb photons from the excitation light to generate electrons and holes. The oscillations of electrons on the surface of Ag particles can enhance the local electromagnetic field. This electromagnetic field not only helps to increase the separation efficiency of electrons and holes but also can make electrons move out of Ag_3PO_4 and quickly to Ag particles due to the high conductivity of Ag. Here, electrons reduce oxygen molecules to form the highly reactive ion O^{2-} [20]. The holes remain on the Ag_3PO_4 surface because the PO_4^{3-} ions have a large negative charge. PO_4^{3-} ions on the surface of Ag_3PO_4 have strong binding ability with H_2O, so H_2O is easily adsorbed on the surface of Ag_3PO_4 and oxidized to OH groups, and will decompose organic matter [21]. That is the reason why Ag/APO samples have higher photocatalytic efficiency than APO.

3. Conclusions

In this study, we have fabricated Ag/Ag_3PO_4 materials in a simple precipitation method with illumination. Observed that Ag particles adhered to Ag_3PO_4 surface through SEM image. Ag/Ag_3PO_4 materials showed higher photocatalytic efficiency than Ag_3PO_4 when decomposing RhB under the same conditions. The Ag/Ag_3PO_4 sample completely decomposed RhB at a concentration of 10 ppm after 15 minutes of illumination with a Xenon lamp. In the survey range, the Ag/Ag_3PO_4 sample reacted to decompose RhB at a concentration of 10 ppm with a reaction rate coefficient 1.35 times higher than that of the Ag_3PO_4 sample under the same conditions.

Acknowledgments. This study was carried out with the support of the Ministry of Education and Training project, code B2020-MDA-11.

REFERENCES

[1] Sui, Z., Q. Meng, X. Zhang, R. Ma, and B. Cao, 2012. Green synthesis of carbon nanotube-graphene hybrid aerogels and their use as versatile agents for water purification. *J. Mater. Chem.*, Vol. 22, pp. 8767-8771.

[2] Zhu, Y.W., S. Murali, W.W. Cai, X.S. Li, J.W. Suk, J.R. Potts, and R.S. Ruoff, 2010. Graphene and graphene oxide: synthesis, properties, and applications. *Adv. Mater.*, Vol. 22, pp. 3906-3924.

[3] Yi, Z., J. Ye, N. Kikugawa, T. Kako, S. Ouyang, H. Stuart-Williams, H. Yang, J. Cao, W. Luo, Z. Li, Y. Liu, and R.L. Withers, 2010. An orthophosphate semiconductor with photooxidation properties under visible-light irradiation. *Nat. Mater.*, Vol. 9, pp. 559-564.

[4] Chen, X., Y. Dai, and X. Wang, 2015. Methods and mechanism for improvement of photocatalytic activity and stability of Ag_3PO_4: A review. *J. Alloys Compd.*, Vol. 649, pp. 910-932.

[5] Huang, G.-F., Z.-L. Ma, W.-Q. Huang, Y. Tian, C. Jiao, Z.-M. Yang, Z. Wan, and A. Pan, 2013. Ag_3PO_4 Semiconductor Photocatalyst: Possibilities and Challenges. *J. Nanomater.*, Vol. 2013, pp. 371356-8.

[6] Liu, Q., N. Li, Z. Qiao, W. Li, L. Wang, S. Zhu, Z. Jing, and T. Yan, 2019. The Multiple Promotion Effects of Ammonium Phosphate-Modified Ag_3PO_4 on Photocatalytic Performance. *Front. Chem.*, Vol. 7, pp. 1-12.

[7] Yan, T., W. Guan, W. Li, and J. You, 2014. Ag_3PO_4 photocatalysts loaded on uniform SiO_{-2} support for efficient degradation of methyl orange under visible light irradiation. *RSC Advances*, Vol. 4, pp. 37095-37099.

[8] Liang, Q., Y. Shi, W. Ma, Z. Li, and X. Yang, 2012. Enhanced photocatalytic activity and structural stability by hybridizing Ag_3PO_4 nanospheres with graphene oxide sheets. *Physical Chemistry Chemical Physics*, Vol. 14, pp. 15657-15665.

[9] Liu, M., G. Wang, P. Xu, Y. Zhu, and W. Li, 2020. Construction of Ag_3PO_4/SnO_2 Heterojunction on Carbon Cloth with Enhanced Visible Light Photocatalytic Degradation. *Applied Sciences*, Vol. 10, pp. 3238.

[10] Zhang, M., H. Du, J. Ji, F. Li, Y.C. Lin, C. Qin, Z. Zhang, and Y. Shen, 2021. Highly Efficient Ag_3PO_4/g-C_3N_4 Z-Scheme Photocatalyst for Its Enhanced Photocatalytic Performance in Degradation of Rhodamine B and Phenol. *Molecules (Basel, Switzerland)*, Vol. 26, pp. 2062.

[11] Osman, N.S., S.N. Sulaiman, E.N. Muhamad, H. Mukhair, S.T. Tan, and A.H. Abdullah, 2021. Synthesis of an Ag_3PO_4/Nb_2O_5 Photocatalyst for the Degradation of Dye. *Catalysts*, Vol. 11, pp. 458.

[12] Panthi, G., K.R. Gyawali, and M. Park, 2020. Towards the Enhancement in Photocatalytic Performance of Ag_3PO_4 Nanoparticles through Sulfate Doping and Anchoring on Electrospun Nanofibers. *Nanomaterials*, Vol. 10, pp. 929.

[13] Xie, Y.P. and G.S. Wang, 2014. Visible light responsive porous Lanthanum-doped Ag_3PO_4 photocatalyst with high photocatalytic water oxidation activity. *J. Colloid Interface Sci.*, Vol. 430, pp. 1-5.

[14] Shi, L., L. Liang, J. Ma, F. Wang, and J. Sun, 2014. Remarkably enhanced photocatalytic activity of ordered mesoporous carbon/*g*-C_3N_4 composite photocatalysts under visible light. *Dalton Transactions*, Vol. 43, pp. 7236-7244.

[15] Febiyanto and U. Sulaeman, 2020. The Starting Material Concentration Dependence of Ag_3PO_4 Synthesis for Rhodamine B Photodegradation under Visible Light Irradiation. *Journal Kimia Valensi*, Vol. 6, pp. 1-8.

[16] Trench, A.B., T.R. Machado, A.F. Gouveia, M. Assis, L.G. Trindade, C.C. Santos, A. Perrin, C. Perrin, M. Oliva, J. Andrés, and E. Longo, 2018. Connecting structural, optical, and electronic properties and photocatalytic activity of Ag_3PO^4:Mo complemented by DFT calculations. *J. Applied Catalysis B-Environmental*, Vol. 238, pp. 198-211.

[17] Botelho, G., J.C. Sczancoski, J. Andres, L. Gracia, and E. Longo, 2015. Experimental and Theoretical Study on the Structure, Optical Properties, and Growth of Metallic Silver Nanostructures in Ag_3PO_4. *J. Phys. Chem. C*, Vol. 119, pp. 6293-6306.

[18] Mroczkowska, M., J.L. Nowinski, G.Z. Zukowska, A. Mroczkowska, J.E. Garbarczyk, M. Wasiucionek, and S. Gierlotka, 2007. Micro Raman, FT-IR/PAS, XRD and SEM studies on glassy and partly crystalline silver phosphate ionic conductors. *Journal of Power Sources*, Vol. 173, pp. 729-733.

[19] Song, L., J. Yang, and S. Zhang, 2017. Enhanced photocatalytic activity of Ag_3PO_4 photocatalyst via glucose-based carbon sphere modification. *Chemical Engineering Journal*, Vol. 309, pp. 222-229.

[20] Yu, J., G. Dai, and B. Huang, 2009. Fabrication and Characterization of Visible-Light-Driven Plasmonic Photocatalyst Ag/AgCl/TiO_2 Nanotube Arrays. *J. Phys. Chem. C*, Vol. 113, pp. 16394-16401.

[21] Liu, Y., L. Fang, H. Lu, Y. Li, C. Hu, and H. Yu, 2012. One-pot pyridine-assisted synthesis of visible-light-driven photocatalyst Ag/Ag_3PO_4. *Appl. Catal. B-Environ.*, Vol. 115-116, pp. 245-252.